

# Composable Strategy Framework with Integrated Video-Text based Large Language Models for Heart Failure Assessment

Jianzhou Chen<sup>a, §</sup>, Jinyang Sun<sup>b, §</sup>, Xiumei Wang<sup>c</sup>, Xi Chen<sup>d</sup>, Heyu Chu<sup>e</sup>, Guo Song<sup>e</sup>, Yuji Luo<sup>e</sup>, Xingping Zhou<sup>f, ‡</sup>, and Rong Gu<sup>a,\*</sup>

<sup>a</sup>*Department of Cardiology, Nanjing Drum Tower Hospital, State Key Laboratory of Pharmaceutical Biotechnology, Nanjing University, Nanjing 210008, China*

<sup>b</sup>*Portland Institute, Nanjing University of Posts and Telecommunications, Nanjing 210003, China*

<sup>c</sup>*College of Electronic and Optical Engineering, Nanjing University of Posts and Telecommunications, Nanjing 210003, China*

<sup>d</sup>*College of Integrated Circuit Science and Engineering, Nanjing University of Posts and Telecommunications, Nanjing 210003, China*

<sup>e</sup>*Department of Cardiology, Nanjing Drum Tower Hospital Clinical College of Nanjing Medical University, Nanjing 210008, China*

<sup>f</sup>*Institute of Quantum Information and Technology, Nanjing University of Posts and Telecommunications, Nanjing 210003, China*

§ These authors contributed equally to this work.

Correspondence: [zxp@njupt.edu.cn](mailto:zxp@njupt.edu.cn)

Correspondence: [gurong.nju@163.com](mailto:gurong.nju@163.com)

---

## Abstract

Heart failure is one of the leading causes of death worldwide, with millions of deaths each year, according to data from the World Health Organization (WHO) and other public health agencies. While significant progress has been made in the field of heart failure, leading to improved survival rates and improvement of ejection fraction, there remains substantial unmet needs, due to the complexity and multifactorial characteristics. Therefore, we propose a composable strategy framework for assessment and treatment optimization in heart failure. This framework simulates the doctor-patient consultation process and leverages multi-modal algorithms to analyze a range of data, including video, physical examination, text results as well as medical history. By integrating these various data sources, our framework offers a more holistic evaluation and optimized treatment plan for patients. Our results demonstrate that this multi-modal approach outperforms single-modal artificial intelligence (AI) algorithms in terms of accuracy in heart failure (HF) prognosis prediction. Through this method, we can further evaluate the impact of various pathological indicators on HF prognosis, providing a more comprehensive evaluation.

---

## 1. Introduction

Heart failure (HF) is a complex and multifactorial disease, and its clinical manifestations, treatment and prevention are widely challenging. With the aging of the population and the increase in cardiovascular disease, the incidence rate of heart failure continues to rise, resulting in a huge consumption of medical resources worldwide. In the treatment of heart failure, lifestyle intervention, pharmacological management, the device-based management, and heart transplantation are the main treatment methods. The addition of a neprilysin inhibitor to renin–angiotensin system inhibition (ARNI), and the advent of SGLT2 inhibition are the main supplemental solutions of pharmacological management [1]. The incidence rate of newly diagnosed heart failure has reportedly stabilized or may even be declining in the general population. People with heart failure also live longer. However, the long-term trend of increasing numbers of individuals at risk for heart failure and increasing survival rates for individuals with heart failure has led to an overall increase in the prevalence of heart failure patients.

On the other hand, the vigorous development of deep learning has brought new paradigms to scientific research in various fields, and it has also been widely used in clinical studies [2]. Deep learning can discover patterns, predict diseases, assist in diagnosis, and optimize treatment plans by analyzing large amounts of medical data, significantly improving medical efficiency. It has played a significant role in medical image analysis [3], clinical decision support [4], clinical data analysis [5], [6], and other fields.

Recent years, scientists employ the machine learning to mine the mapping relationship connected with HF between various important factors such as subclinical hypothyroidism [7], clonal hematopoiesis of indeterminate potential (CHIP), extended somatic variants (ExSV) [8]. This method was also used to predict the composite outcome of HF hospitalization and cardiovascular (CV) death [9], [10]. The machine learning has achieved very good results in the study of HF. However, most of these works focus on the influence of single factor on HF [7]-[16], which may lead to inaccurate and partial judgment.

Fortunately, multimodal artificial intelligence (AI) refers to AI systems that can simultaneously process and understand data from multiple different modalities (such as text, images, audio, video, etc.) [17]-[27]. Compared with traditional single-modal AI systems, multi-modal AI can better simulate human perception and integrate different types of information. This technology was quickly applied to the clinical studies, such as Alzheimer's disease dementia assessment [18], [21], neuroprognosis performance in clinically unresponsive critical-care patients with brain injury [19], identification of clinical disease trajectories in neurodegenerative disorders [6], etc.

In our work, we propose the Multimodal Post-Recovery Tracking Model (M-PRTM), a framework that integrates cinematic, numerical, and textual data to improve HF prognosis prediction. M-PRTM combines clinical data such as patient demographics, clinical metrics, and medication history with Cardiac Magnetic Resonance (CMR) images to create a comprehensive model. Our framework employs specialized models for each data modality, including the DAE-Former for cinematic data, a fully connected network for numerical data, and a BERT-based model for textual data. These features are then fused using an attention mechanism, which dynamically prioritizes the most important information for predictions, such as drug prescriptions and vital signs. Our results show that M-PRTM achieves 96.5% accuracy in predicting clinical outcomes, outperforming traditional single-modal approaches, and demonstrating its ability to handle complex, multimodal data for more reliable patient predictions. The framework's ability to dynamically adjust the importance of each modality enables more accurate predictions, while its multimodal nature supports personalized treatment strategies and early intervention. Through rigorous testing with data from 136 and 688 patients, M-PRTM demonstrates its effectiveness in prediction of HF prognosis, offering a scalable solution for optimizing patient care and improving outcomes.

## 2. Overview and results

### 2.1. M-PRTM's Overview

The comprehensive workflow for M-PRTM's development and validation is presented in Fig. 1. Additionally, we have described the underlying structure that supports the data modalities as well. In the Data column, patient data are categorized into three main types: numerical indicators, textual prescriptions, and CMR cinematic data. Numerical indicators include demographic information (e.g., gender and age) and key clinical metrics (e.g., blood pressure and BMI). Textual records primarily consist of prescription information, such as drug type, dosage, and treatment stage. Meanwhile, CMR imaging data capture anatomical and functional features of the myocardium, including regions of fibrosis. In particular, Late Gadolinium Enhancement (LGE) is a key imaging biomarker for detecting myocardial fibrosis. It provides crucial insights into the structural integrity and scarring of the myocardium, which are closely linked to the progression of HF [28], [29]. To leverage these imaging insights, we extract vector features from numerical, textual, and CMR cinematic data for multimodal fusion-based predictions. Specifically, we provide an example in the Medical Prescription section. Considering that drug types and dosages often vary across time or treatment stages during clinical practice, our data processing accounts for these dynamic changes to enhance the M-PRTM's adaptability to patient medication patterns.

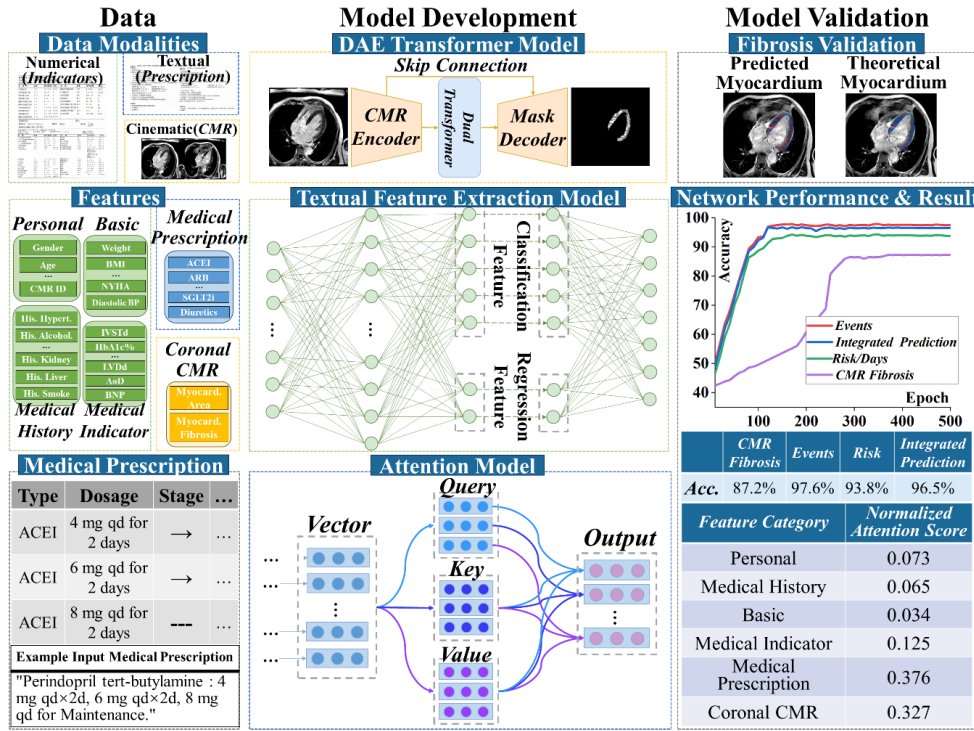


**Fig. 1.** Overview of data, model development, and model validation.

The Model Development column outlines three modules designed to process imaging, numerical, and textual tasks. For imaging data, we employ the Dual Attention-guided Efficient Transformer model (DAE-

former) [30]. The model integrates a skip-connected CMR encoder and masked decoder, which enable precise predictions of myocardial fibrosis regions and can significantly improve segmentation accuracy. For the numerical type data, we construct a feature extraction model to map the numerical inputs into classification and regression features. Those features are further refined using an Attention Model, which calculates the "Query-Key-Value" weights to highlight critical attributes impacting prediction outcomes. For the textual type data, we apply a pre-trained Bidirectional Encoder Representations from Transformers (BERT) model [31], [32] to embed textual information. It is complemented by an Attention Model to dynamically adjust the importance of textual features, effectively capturing the impact of phased drug adjustments on prediction outcomes.

In the Model Validation step, the Fibrosis Validation module evaluates the predicted fibrosis regions, showing high consistency between the prediction results and the theoretical annotations. This demonstrates the accuracy and efficacy of the model in fibrosis segmentation. Additionally, the Network Performance & Result curves illustrate the model's accuracy across multiple prediction tasks, including fibrosis segmentation, event prediction, risk prediction, and integrated prediction, achieving 87.2%, 97.6%, 93.8%, and 96.5%, respectively. Finally, feature importance analysis reveals that therapeutic agents and CMR cinematic data contribute the most to the predictions, with importance scores of 0.376 and 0.327, respectively. Other feature categories, such as numerical indicators and medical indicator, also make contributions but with lower importance scores.

Overall, the validation results can confirm that our multimodal framework effectively integrates CMR, numerical type, and textual type data, enabling highly accurate and reliable predictions of clinical outcomes. This highlights the potential of the M-PRTM to support personalized medicine and optimize patient management strategies.

## 2.2. M-PRTM's Performance and Results

In this section, we present key performance metrics of the proposed M-PRTM alongside its prediction results. By visualizing the training and testing processes, we provide an intuitive demonstration of the model's efficiency and accuracy. The training process of the DAE-former is shown in Fig. 2(a), where the Dice Similarity Coefficient (DSC) and Harsdorf Distance (HD) are plotted against the number of epochs. Additionally, we present examples of predicted Myocardial Fibrosis regions alongside their corresponding ground truth labels, as shown in Fig. 2(b). The results indicate that the fibrosis regions predicted by DAE-former closely align with manual annotations, achieving an accuracy of approximately 87%, demonstrating the model's effectiveness in processing imaging data. A key contribution of our work is the design and implementation of the M-PRTM, which is specifically developed to integrate textual, numerical, and cinematic data for joint training. The training process of M-PRTM is illustrated in Fig. 2(c), where the test loss and accuracy curves are plotted against epochs. The results show that M-PRTM converges rapidly, with the test loss gradually decreasing and test accuracy steadily increasing, which demonstrates its effectiveness in processing multimodal data. The detailed algorithm flowchart for M-PRTM can be found in Fig. 4. To further validate the predictive capabilities of M-PRTM, we present examples of predictions for key clinical outcomes, including mortality, causes of death, days to rehospitalization, and MACCES-related events, as shown in Fig. 2(d). The results reveal strong alignment between predicted values and ground truth, highlighting the ability to handle incomplete recovery data and accurately predict patient outcomes. Furthermore, M-PRTM provides early recommendations for days to rehospitalization or follow-up visits, helping to prevent unnecessary mortality caused by deteriorating conditions during recovery. Fig. 2(e) highlights the unique functionality of M-PRTM in dynamically assessing patient risk and predicting recovery prognosis.

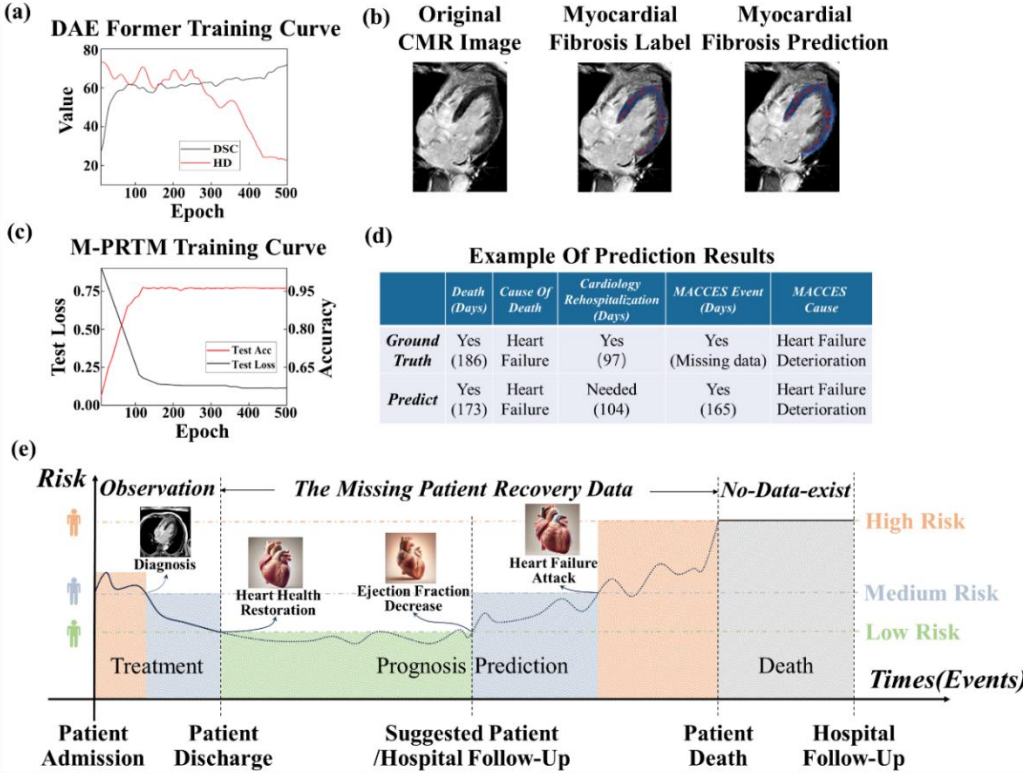


**Fig. 2.** Model Performance and Prediction Results. (a) Training curves of the DAE-former model showing the DSC and HD across 500 epochs. (b) Example of Myocardial Fibrosis prediction results. The original CMR image, ground truth label, and predicted fibrosis region show strong alignment with an accuracy of approximately 87%. (c) Training curves of the proposed M-PRTM model showing the test loss and acc across 500 epochs. (d) Prediction examples of clinical outcomes, including death, cause of death, rehospitalization days, and MACCES events. (e) Timeline of patient risk stratification and recovery prognosis. The model dynamically assesses risks and predicts critical events, such as HF recovery and ejection fraction decline.

By integrating multimodal data, the M-PRTM evaluates patient risk at different stages and forecasts critical events. For instance, during the treatment phase, it identifies the recovery time point for HF (green low-risk region). As the patient transitions to the follow-up stage post-discharge, potential risks such as declining ejection fraction (blue medium-risk region) begin to emerge. The M-PRTM further predicts high-risk events, such as HF deterioration (orange high-risk region), and intelligently infers risk trends during data-absent follow-up windows based on historical data. This mechanism, depicted in Fig. 2(e), demonstrates the capability of M-PRTM to support personalized follow-up strategies. It provides tailored recommendations for re-evaluation and follow-up visits, reducing unnecessary medical burdens for low-risk patients while optimizing resources and offering scientific guidance for precise interventions.

### 2.3. M-PRTM's Evaluation and Analysis

In this section, we evaluate the performance of the proposed M-PRTM under different modality combinations and analyze the impact of attention allocation strategies. When integrating textual, cinematic, and numerical modalities, the M-PRTM achieves a maximum accuracy of 96.5%, indicating that combining

multimodal data significantly enhances predictive performance. When using only two modalities, the combination of textual and cinematic modalities achieves an accuracy of 94.0%, outperforming the combinations of textual and numerical modalities (92.5%) and cinematic and numerical modalities (86.5%), as shown in Fig. 3(a). This highlights the critical role of the textual modality, as it contains prescription information from physicians, which is pivotal for subsequent predictions.

**Table 1.** Performance of Modal Combinations and Attention Allocation Strategies

Modal combination	Acc%	Attention allocation	Acc%
Textual + Cinematic + Numerical	96.5	Self-attention	96.5
Textual + Cinematic	94.0	Text 50% + Cine 25% + Num 25%	91.7
Textual + Numerical	92.5	Text 25% + Cine 50% + Num 25%	87.7
Cinematic + Numerical	86.5	Text 25% + Cine 25% + Num 50%	84.8

We further investigate the impact of different attention allocation strategies on model performance, as depicted in Fig. 3(b). The Self-Reasoning Attention mechanism delivers the highest accuracy of 96.5%, demonstrating its effectiveness in balancing the contributions of each modality to the predictions. Under fixed weight allocation strategies, the M-PRTM achieves an accuracy of 91.7% when assigning 50% weight to the textual modality, 25% to the cinematic modality, and 25% to the numerical modality. In contrast, assigning 25% weight to the textual modality, 50% to the cinematic modality, and 25% to the numerical modality results in a lower accuracy of 87.7%. Assigning 50% weight to the numerical modality produces the lowest accuracy, at only 84.8%. These results demonstrate that adaptive attention allocation strategies optimize the synergy among modalities and fully leverage the strengths of different data types.

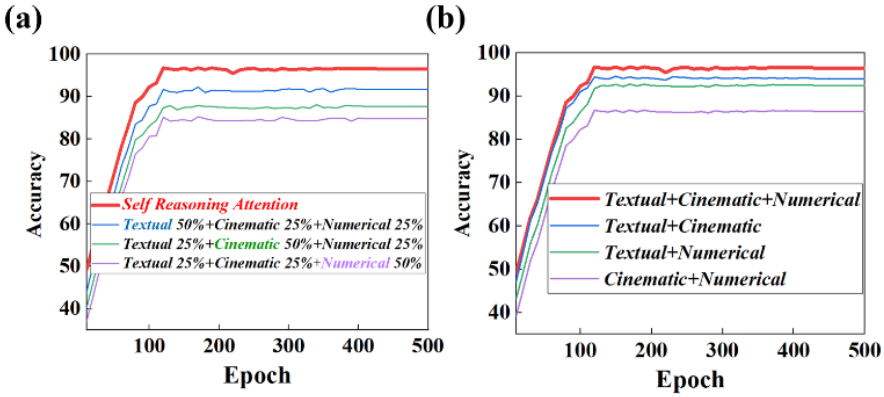


**Fig. 3.** Model Performance with Attention Allocation and Modal Combinations. (a) Accuracy comparison for different modal combinations. The combination of textual, cinematic, and numerical data achieves the highest accuracy, followed by textual and cinematic data. (b) Accuracy comparison under different attention allocation strategies. Self-Reasoning Attention achieves the best performance, outperforming fixed weight allocations.

The analysis indicates that the textual data plays a dominant role in predictions, as it contains critical information such as phased prescription adjustments. In contrast, numerical data such as personal and basic metrics tends to diminish the importance of features like medical history. Consequently, its contribution to the M-PRTM's attention allocation is relatively lower. Ultimately, our Self-Reasoning Attention mechanism allocates approximately 55% to textual data, 30% to cinematic data, and 15% to numerical data. These

findings further highlight the significant variation in contributions among modalities, underscoring the necessity of dynamic allocation strategies to optimize balance and maximize the model performance.

### 3. Data Collection and Processing

Our research focuses on HF prognosis prediction and myocardial fibrosis detection. It utilizes data from 136 and 688 patients, comprising CMR cinematic data and clinical information respectively. The clinical data encompass demographic details and key clinical indicators, with baseline characteristics detailed in Table 2. We have also outlined the preprocessing methods for cinematic, textual, and numerical data. Ethical approval for this study was granted by the Ethics Committee of Nanjing Drum Tower Hospital (Approval No. 2025-0094-015).

**Table 2.** Baseline Characteristics and Key Clinical Indicators

Column Name	Mode Type	Mean	Standard Deviation	Range
Gender	Numerical	0.8014	0.4003	(0,1)
Age	Numerical	52.367	14.391	(18,79)
Weight	Numerical	73.006	16.877	(42.0,121.2)
Heart Rate (bpm)	Numerical	85.602	19.331	(43,153)
...	...	...	...	...
Diastolic BP	Numerical	85.242	18.890	(39,144)
Myocardial Infarction	Numerical	0.1176	0.3233	(0,1)
Pacemaker	Numerical	0.0441	0.2061	(0,1)
Medical Indicator	Text	—	—	—
IVSTd	Numerical	0.9391	0.2253	(0.5,1.87)
ALT	Numerical	38.265	42.408	(5.3,340.8)
AST	Numerical	30.633	26.288	(10.8,235)
Albumin/Globulin Ratio	Numerical	1.6280	0.2911	(0.76,2.32)
...	...	...	...	...
LDL-C	Numerical	2.5078	0.9104	(0.46,5.07)
Apo-A1	Numerical	0.9065	0.2043	(0.46,1.63)
HbA1c%	Numerical	6.2455	1.1636	(4.3,11.3)

#### 3.1. Cinematic Data

All CMR cinematic data are standardized in spatial resolution and uniformly scaled to a size of  $512 \times 512 \times 16$  pixels. To mitigate intensity variations, the intensity values are normalized to ensuring consistent preprocessing standards across all samples.

#### 3.2. Textual Data

A Transformer-based tokenizer is used for encoding. The BERT tokenizer tokenizes textual data, truncating or padding all text to a fixed length of 512 tokens for consistency. Additionally, an attention mask

is generated to handle texts of varying lengths. The encoded textual features are then converted into tensors for the input.

### 3.3. Numerical Data

The median is used to impute missing values, minimizing the influence of extreme values. Subsequently, all numerical features are scaled to the range from 0 to 1, using Min-Max normalization, ensuring equal weighting of different features during training. To address class imbalance in minority case data, an under-sampling strategy is applied. This approach enhances the model's focus on minority class samples, resulting in a more balanced data distribution and improved predictive performance for minority categories while maintaining overall stability.

## 4. M-PRTM Architecture

Our research establishes a multimodal feature extraction and fusion framework. The proposed method integrates the characteristics of cinematic, textual, and numerical data, introducing the targeted data processing workflows and the model structures, as illustrated in Fig. 4. The methodology includes three main stages: data collection, single-modal feature extraction (cinematic features, numerical features, and textual features), and multimodal feature fusion.

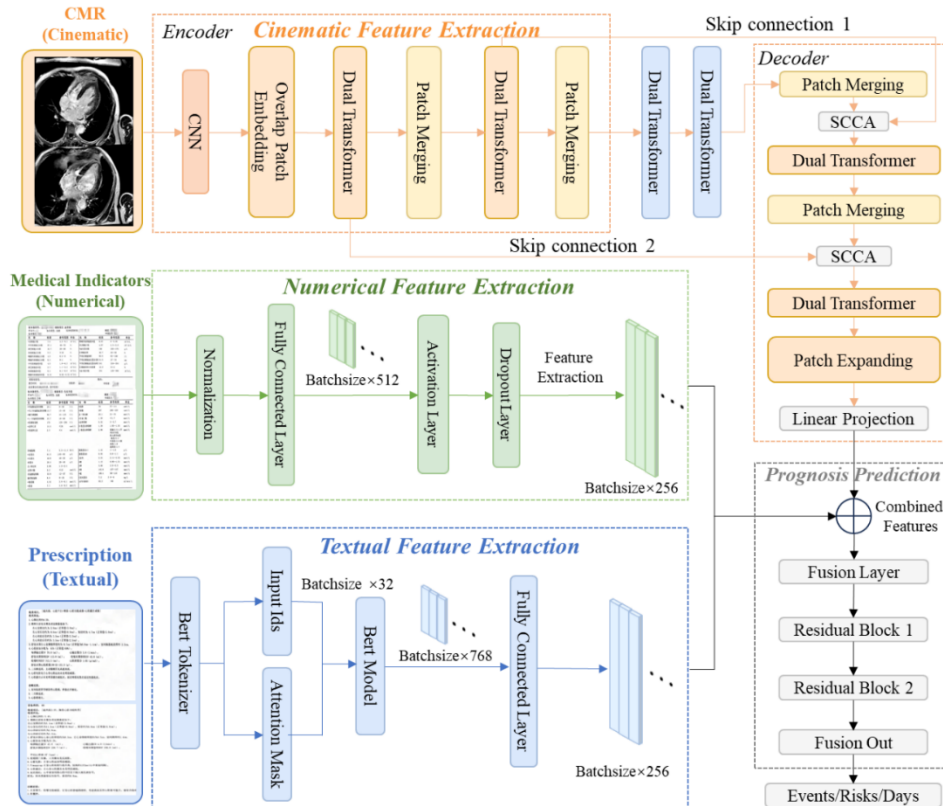


**Fig. 4.** Framework of Multimodal Feature Extraction and Fusion. The diagram illustrates the feature extraction process for cinematic,

numerical, and textual data, followed by multimodal feature fusion. Cinematic features are extracted using the DAE-Former with dual attention and skip connections, numerical features are processed through fully connected layers, and textual features are encoded using BERT. The extracted features are fused through a fusion layer and residual blocks to predict prognosis outcomes such as events, risks, and follow-up days.

#### 4.1. Cinematic Feature Extraction Module

In myocardial fibrosis detection tasks, we employ the DAE-Former model [30]. DAE is a pure Transformer architecture designed specifically for medical image segmentation. It addresses the limitations of traditional convolutional neural networks (CNNs) in capturing long-range dependencies and global contextual information while overcoming the high computational complexity of standard Transformers.

As illustrated in the imaging processing workflow in Fig. 4, DAE-Former consists of an input encoder, output encoder, Efficient Dual Attention (Efficient Attention and Transpose Attention), Skip Connection Cross Attention (SCCA), and an output layer. The core components of Efficient Dual Attention and SCCA are detailed in Fig. 5 with their structural diagrams.

The EDA module is a dual Transformer block that integrates transposed (channel) attention and effective (spatial) attention, as shown in Fig. 5(a). This dual-attention block integrates effective attention, normalization, and transposed attention block that performs channel attention. Fig. 5(b) presents the structure of another key module SCCA, which employs a cross-processing approach to more effectively preserve low-level features. This module is capable of providing spatial information that helps recover fine-grained details when generating the output mask. Specifically, SCCA incorporates an effective attention mechanism. Its query input is derived from the encoder layer output forwarded through the skip connection, while the keys and values originate from the lower decoder layer. To integrate these two features, a linear layer is employed to scale to match the embedding dimension. The rationale for using as the query input is to model multi-level representations within the effective attention block.

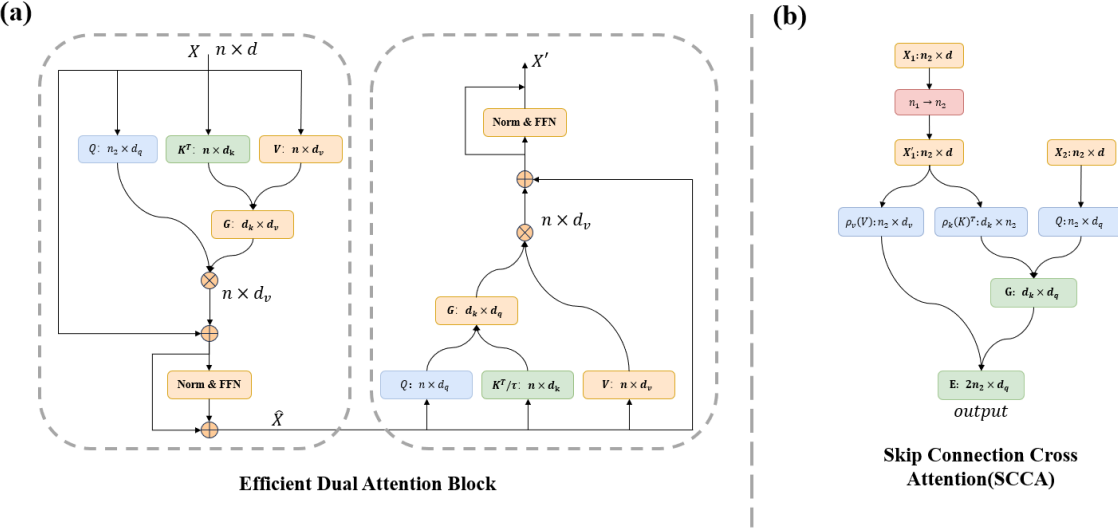


**Fig. 5.** (a) Structure of the Efficient Dual Attention (EDA) module. (b) Structure of the Skip Connection Cross Attention (SCCA) module.

#### 4.2. Efficient Dual Attention

Efficient Dual Attention combines Efficient Attention (to capture spatial information) and Transpose Attention (to capture channel information), enhancing the model's ability to comprehend contextual features. These two mechanisms are applied sequentially, with normalization and residual connections incorporated to improve stability.

#### 4.3. Skip Connection Cross Attention

Skip Connection Cross Attention (SCCA) introduces a cross-attention mechanism into the traditional U-Net architecture. It adaptively fuses encoder features with decoder low-level features, enabling seamless integration of encoder and decoder representations. This process involves linear projection and efficient attention fusion methods, which enhance the recovery of segmentation boundaries and fine details.

For myocardial fibrosis feature extraction from CMR cinematic images, the raw coronal CMR images are first analyzed frame by frame. Myocardial regions, fibrosis shadow regions, and other areas are segmented into different masks. The CMR images, matched with their corresponding masks, are then fed into the DAE-Former network. The M-PRTM identifies potential lesion areas within individual frames and tracks their consistency across multiple slices, leveraging the attention mechanisms inherent in Transformers. Consequently, our M-PRTM can generate stable and accurate predictions of lesion regions, with the ability to capture changes in lesion positions across consecutive frames.

#### 4.4. Numerical Feature Extraction Module

In the numerical tasks, a fully connected layer is designed to process patients' clinical numerical indicators, as illustrated in Fig. 4. The preprocessed numerical features are input into a fully connected network for deep feature extraction. The first layer maps the normalized input data into a 512-dimensional intermediate feature space, incorporating a ReLU activation function to introduce non-linearity. To prevent overfitting, a Dropout layer with a dropout rate of 0.2 is added after the first layer. The second layer further reduces the intermediate features to 256 dimensions to standardize the feature size, facilitating convenient input for subsequent multimodal feature fusion. The final output is a feature tensor with a size of  $\text{batchsize} \times 256$ , consistent with features from other modalities.

#### 4.5. Textual Feature Extraction Module

In this module, a pre-trained BERT model is employed to extract deep semantic features from the textual data. BERT can effectively capture the semantic relationships among words within a sentence, leveraging its strong contextual understanding capabilities. It constructs a comprehensive and accurate representation of textual features, which also enriches the predictive model with semantic insights.

As shown in Fig. 4, textual input is first processed through the BERT tokenizer. Patients' medical histories and medication records are integrated into natural language sentence forms and input into the BERT model for embedding. During this process, BERT utilizes its multi-layer bidirectional Transformer structure to parse the input text word by word, extracting dynamic semantic relationships for each word within its context. The model outputs a global feature vector that encapsulates the overall semantic information of the text, including key clinical details such as drug types and dosage adjustments.

To further enhance the expressiveness of textual features and align them with features from other modalities, a fully connected layer is added after the BERT model's output layer. This layer is designed to

reduce dimensionality, mapping the 768-dimensional semantic vector to a 256-dimensional feature space. This dimensionality reduction not only decreases computational complexity but also ensures dimensional consistency with image and numerical features during the feature fusion stage. Besides, the step optimizes the representation of textual features, retaining original semantic information while improving computational efficiency.

#### 4.6. Multimodal Feature Fusion

We adopt a multimodal fusion strategy incorporating an attention mechanism to integrate features from cinematic, textual, and numerical modalities. To implement this, we design a fusion process that consists of two stages: independent modality feature extraction and multimodal feature fusion, as depicted in Fig. 4.

In the feature extraction stage, unique features are independently extracted from each modality through dedicated modules. Cinematic data are processed by the DAE-Former model, capturing spatial and temporal information at the frame level. Textual data are processed by the BERT model, extracting semantic features to analyze medical histories and medication records. Numerical data are aggregated using a multi-layer perceptron (MLP) to represent clinical indicators. These modules ensure efficient learning of features within their respective spaces.

In the fusion stage, the model dynamically assigns weights to different modality features using an attention mechanism. Specifically, the features of each modality generate Query, Key, and Value matrices, which are used to calculate attention scores across modalities. These scores are scaled and transformed into probability distributions through the SoftMax function, which serves as weights for the feature fusion process. The weighted features are then combined into contextual features. This dynamic process evaluates the contribution of each modality, emphasizing features that are more critical for prediction tasks. Additionally, the fusion strategy incorporates cross-modality regulation, enabling the interaction of information between modalities to optimize feature representation collaboratively. For example, cinematic features can enhance the semantic representation of textual features, while textual features can improve the interpretation of numerical features. This dynamic interaction across modalities significantly boosts the expressiveness of fused features. Finally, the fused features are integrated through a linear layer to generate a unified feature representation for disease and mortality cause prediction. This multimodal fusion strategy not only leverages complementary information from different modalities but also achieves efficient predictive performance, providing essential support for personalized treatment strategies.

### 5. Conclusion

#### 5.1. Methodological Innovations

In this study, we introduce the M-PRTM, a Composable Strategy Framework for HF prognosis that leverages multimodal clinical intelligence. Our model integrates three primary data modalities: numerical indicators, textual prescriptions, and CMR cinematic data. Each modality is processed using specialized architectures, with the DAE-Former for cinematic data, a fully connected network for numerical data, and a BERT-based model for textual data. These representations are fused through an adaptive attention mechanism [33], [34] that dynamically prioritizes critical features, such as drug prescriptions and vital signs. The model achieves an accuracy of 96.5% in HF prognosis prediction, highlighting the benefits of multimodal integration for clinical decision support.

Our findings reveal several key insights into the role of multimodal data in HF assessment. The fusion of textual, numerical, and imaging data provides a more comprehensive evaluation of patient status,

compensating for the limitations of single-modality approaches. Notably, textual prescription data proves essential in predicting clinical outcomes, particularly in forecasting rehospitalization risk and determining optimal follow-up strategies. The framework captures treatment trends that significantly influence patient recovery by analyzing longitudinal drug usage patterns. Additionally, the DAE-Former model processes CMR data to enhance myocardial fibrosis detection, which serves as a key prognostic factor for declining heart function. Multimodal data integration improves predictive accuracy and supports personalized treatment, highlighting the value of cross-domain feature fusion in medical diagnostics.

### *5.2. Clinical Impact*

The integration of multimodal data holds great promise for optimizing clinical management, particularly in complex cases like heart failure. The model's dynamic prioritization of critical features, such as drug prescriptions and vital signs, supports personalized treatment strategies and enables early intervention. By accurately predicting key clinical outcomes such as rehospitalization risk and myocardial fibrosis progression, the M-PRTM can facilitate better resource allocation, reducing unnecessary follow-up visits for low-risk patients while guiding timely interventions for high-risk individuals. In particular, the model's ability to predict the course of myocardial fibrosis, a key prognostic factor for heart failure, positions it as a valuable tool in the clinical evaluation of heart failure patients.

### *5.3. Challenges and Future Directions*

Despite its strong performance, certain limitations in the dataset may affect the M-PRTM's generalizability. The dataset used in this study originates from a single medical institution, which may not fully represent the diversity of patient populations across different geographical and clinical settings. Expanding the dataset to include multi-center cohorts with broader demographic and pathological variations is essential to improve the robustness. Additionally, challenges related to data quality, such as missing values, inconsistent clinical records, and variations in imaging protocols, should be addressed. Future work should focus on implementing advanced preprocessing techniques and data augmentation strategies to mitigate these issues. Furthermore, refining the M-PRTM's ability to handle incomplete data will be crucial for its real-world applicability in heterogeneous clinical environments.

While our framework demonstrates high predictive performance, its interpretability remains a challenge, particularly given the complexity of deep learning-based clinical models. The "black box" nature of neural networks poses obstacles for clinical adoption, as medical professionals require transparency in decision-making. Although our attention mechanism dynamically adjusts modality importance, further efforts are necessary to enhance the explainability. Future work should explore post-hoc interpretability methods and integrate expert-driven validation, such as comparisons with cardiologist assessments, may further enhance trust and acceptance in real-world clinical settings.

Looking ahead, the M-PRTM framework shows great potential beyond HF prognosis. Its integration of video, textual, and numerical data allows adaptation to other medical fields, such as oncology, diabetes management, and neurodegenerative disease monitoring. In resource-limited settings, where advanced imaging may be less accessible, the model's reliance on textual and numerical data still enables highly accurate predictions, expanding its applicability. As multimodal data collection and AI methodologies continue to evolve, frameworks like M-PRTM are expected to transform clinical decision support, driving the future of precision medicine and personalized healthcare.

## Acknowledgements

This work was supported by the National Natural Science Foundation of China under Grant 12404365. Ethical approval was granted by the Ethics Committee of Nanjing Drum Tower Hospital (Approval No. 2025-0094-015). The authors thank Professor Xiaofei Li for insightful discussions.

## References

- [1] C.S. Lam, K.F. Docherty, J.E. Ho, J.J. McMurray, P.L. Myhre, T. Omland, Recent successes in heart failure treatment, *Nat. Med.* 29 (10) (2023) 2424–2437.
- [2] P. Rajpurkar, E. Chen, O. Banerjee, E.J. Topol, AI in health and medicine, *Nat. Med.* 28 (1) (2022) 31–38.
- [3] D. Shen, G. Wu, H.I. Suk, Deep learning in medical image analysis, *Annu. Rev. Biomed. Eng.* 19 (1) (2017) 221–248.
- [4] S. Tayebi Arasteh, T. Han, M. Lotfinia, C. Kuhl, J.N. Kather, D. Truhn, S. Nebelung, Large language models streamline automated machine learning for clinical studies, *Nat. Commun.* 15 (1) (2024) 1603.
- [5] X. Chen, X. Wang, K. Zhang, K.-M. Fung, T.C. Thai, K. Moore, R.S. Mannel, H. Liu, B. Zheng, Y. Qiu, Recent advances and clinical applications of deep learning in medical image analysis, *Med. Image Anal.* 79 (2022) 102444.
- [6] N.J. Mekkes, M. Groot, E. Hoekstra, A. de Boer, E. Dagkesamanskaia, S. Bouwman, S.M. Wehrens, M.K. Herbert, D.D. Wever, A. Rozemuller, others, Identification of clinical disease trajectories in neurodegenerative disorders with natural language processing, *Nat. Med.* 30 (4) (2024) 1143–1153.
- [7] R. Yagi, C. Macrae, R.C. Deo, S. Goto, A Deep Learning Electrocardiogram Model Identifies Risk of Incident Heart Failure in Patients With Subclinical Hypothyroidism, *Circulation* 148 (2023) A16324–A16324.
- [8] N. Chen, M. Shen, V. Rao, J. Ivey Miranda, Z. Tan, W. Wei, J.M. Testani, S. Halene, J. Gu, H. Zhao, others, Novel Partition Scores Identify Pathways Implicated in Clonal Hematopoiesis of Indeterminate Potential (CHIP) Mediated Heart Failure, *Circulation* 148 (2023) A17773–A17773.
- [9] E.D. Adler, A.A. Voors, L. Klein, F. Macheret, O.O. Braun, M.A. Urey, W. Zhu, I. Sama, M. Tadel, C. Campagnari, others, Improving risk prediction in heart failure using machine learning, *Eur. J. Heart Fail.* 22 (1) (2020) 139–147.
- [10] M.W. Segar, M.S. Usman, K.V. Patel, M.S. Khan, J. Butler, L. Manjunath, C.S. Lam, S. Verma, D. Willett, D. Kao, others, Development and validation of a machine learning-based approach to identify high-risk diabetic cardiomyopathy phenotype, *Eur. J. Heart Fail.* 26 (10) (2024) 2183–2192.
- [11] E.S. Lau, P. Di Achille, K. Kopparapu, C.T. Andrews, P. Singh, C. Reeder, M. Al-Alusi, S. Khurshid, J.S. Haimovich, P.T. Ellinor, others, Deep learning–enabled assessment of left heart structure and function predicts cardiovascular outcomes, *J. Am. Coll. Cardiol.* 82 (20) (2023) 1936–1948.
- [12] L. Monzo, E. Bresso, K. Dickstein, B. Pitt, J.G. Cleland, S.D. Anker, C.S. Lam, M.R. Mehra, D.J. van Veldhuisen, B. Greenberg, others, Machine learning approach to identify phenotypes in patients with ischaemic heart failure with reduced ejection fraction, *Eur. J. Heart Fail.* (2024).
- [13] H.S. Lumish, N. Harano, L.W. Liang, K. Hasegawa, M.S. Maurer, A. Tower-Rader, M.A. Fifer, M.P. Reilly, Y.J. Shimada, Prediction of new-onset atrial fibrillation in patients with hypertrophic cardiomyopathy using plasma proteomics profiling, *Europace* 26 (11) (2024) euae267.
- [14] E. Kokori, R. Patel, G. Olatunji, B.M. Ukoaka, I.C. Abraham, V.O. Ajekigbe, J.M. Kwape, A.E. Babalola, N.G. Udam, N. Aderinto, Machine learning in predicting heart failure survival: a review of current models and future prospects, *Heart Fail. Rev.* 30 (2) (2025) 431–442.

[15] A.M. Flores, F. Demasas, N.J. Leeper, E.G. Ross, Leveraging machine learning and artificial intelligence to improve peripheral artery disease detection, treatment, and outcomes, *Circ. Res.* 128 (12) (2021) 1833–1850.

[16] K. Ma, J. Yang, Y. Shao, P. Li, H. Guo, J. Wu, Y. Zhu, H. Zhang, X. Zhang, J. Du, others, Therapeutic and prognostic significance of arachidonic acid in heart failure, *Circ. Res.* 130 (7) (2022) 1056–1071.

[17] S. Yin, C. Fu, S. Zhao, K. Li, X. Sun, T. Xu, E. Chen, A survey on multimodal large language models, *Natl. Sci. Rev.* 11 (12) (2024) nwae403.

[18] S. Qiu, et al., Multimodal deep learning for Alzheimer's disease dementia assessment, *Nat. Commun.* 13 (1) (2022) 3404.

[19] B. Rohaut, C. Calligaris, B. Hermann, P. Perez, F. Faugeras, F. Raimondo, J.-R. King, D. Engemann, C. Marois, L. Le Guennec, others, Multimodal assessment improves neuroprognosis performance in clinically unresponsive critical-care patients with brain injury, *Nat. Med.* 30 (8) (2024) 2349–2355.

[20] C. Xue, S.S. Kowshik, D. Lteif, S. Puducher, V.H. Jasodanand, O.T. Zhou, A.S. Walia, O.B. Guney, J.D. Zhang, S. Poésy, others, AI-based differential diagnosis of dementia etiologies on multimodal data, *Nat. Med.* 30 (10) (2024) 2977–2989.

[21] H. Zhou, L. He, B.Y. Chen, L. Shen, Y. Zhang, Multi-modal diagnosis of Alzheimer's disease using interpretable graph convolutional networks, *IEEE Trans. Med. Imag.* 44 (1) (2025) 142–153.

[22] Y. Oh, S. Park, H.K. Byun, Y. Cho, I.J. Lee, J.S. Kim, J.C. Ye, LLM-driven multimodal target volume contouring in radiation oncology, *Nat. Commun.* 15 (1) (2024) 9186.

[23] S. Tayebi Arasteh, T. Han, M. Lotfinia, C. Kuhl, J.N. Kather, D. Truhn, S. Nebelung, Large language models streamline automated machine learning for clinical studies, *Nat. Commun.* 15 (1) (2024) 1603.

[24] S. Volinsky-Fremond, et al., Prediction of recurrence risk in endometrial cancer with multimodal deep learning, *Nat. Med.* 30 (7) (2024) 1962–1973.

[25] M.Y. Lu, B. Chen, D.F. Williamson, R.J. Chen, M. Zhao, A.K. Chow, K. Ikemura, A. Kim, D. Pouli, A. Patel, others, A multimodal generative AI copilot for human pathology, *Nature* 634 (2024) 466–473.

[26] J. Klughammer, D.L. Abravanel, Å. Segerstolpe, T.R. Blosser, Y. Goltsev, Y. Cui, D.R. Goodwin, A. Sinha, O. Ashenberg, M. Slyper, others, A multi-modal single-cell and spatial expression map of metastatic breast cancer biopsies across clinicopathological features, *Nat. Med.* 30 (11) (2024) 3236–3249.

[27] J. Li, Z. Guan, J. Wang, C.Y. Cheung, Y. Zheng, L.L. Lim, C.C. Lim, P. Ruamviboonsuk, R. Raman, L. Corsino, others, Integrated image-based deep learning and language models for primary diabetes care, *Nat. Med.* 30 (10) (2024) 2886–2896.

[28] J.A. Gonzalez, C.M. Kramer, Role of imaging techniques for diagnosis, prognosis and management of heart failure patients: cardiac magnetic resonance, *Curr. Heart Fail. Rep.* 12 (4) (2015) 276–283.

[29] B. López, S. Ravassa, M.U. Moreno, G.S. José, J. Beaumont, A. Gonzalez, J. Díez, Diffuse myocardial fibrosis: mechanisms, diagnosis and therapeutic approaches, *Nat. Rev. Cardiol.* 18 (7) (2021) 479–498.

[30] R. Azad, R. Arimond, E.K. Aghdam, A. Kazerouni, D. Merhof, Dae-former: Dual attention-guided efficient transformer for medical image segmentation, in: *Int. Workshop Predict. Intell. Med.*, Springer, 2023: pp. 83–95.

[31] J. Devlin, M.W. Chang, K. Lee, K. Toutanova, BERT: Pre-training of deep bidirectional transformers for language understanding, in: *Proc. 2019 Conf. North Am. Chapter Assoc. Comput. Linguist. Human Lang. Technol.*, 2019: pp. 4171–4186.

[32] M.V. Koroteev, BERT: a review of applications in natural language processing and understanding, *ArXiv Preprint ArXiv:2103.11943* (2021).

- [33] S. Sukhbaatar, E. Grave, P. Bojanowski, A. Joulin, Adaptive Attention Span in Transformers, in: A. Korhonen, D. Traum, L. Márquez (Eds.), Proc. 57th Annu. Meet. Assoc. Comput. Linguist., Assoc. Comput. Linguist., Florence, Italy, 2019: pp. 331–335.
- [34] S. Liu, T. Lin, D. He, F. Li, M. Wang, X. Li, Z. Sun, Q. Li, E. Ding, Adaattn: Revisit attention mechanism in arbitrary neural style transfer, in: Proc. IEEE/CVF Int. Conf. Comput. Vision, 2021: pp. 6649–6658.